Ligand-Field Calculations on Pseudo-Tetragonal High-Spin Fe(II) Compounds

Part II: Interpretation of experimental magnetic susceptibility, magnetic saturation, Mössbauer spectra, and ligand-field spectra in a single model

A. Vermaas, W. L. Groeneveld

Department of Coordination Chemistry, State University, P.O. Box 75, Leiden
The Netherlands

and

J. Reedijk

Department of Chemistry, Delft University of Technology, Julianalaan 136, Delft
The Netherlands

(Z. Naturforsch. **32a**, 1404–1418 [1977]; received October 18, 1977)

The compounds $Fe(pz)_4X_2$ and $Fe(mpz)_4X_2$, where pz stands for pyrazole, mpz for 5-methylpyrazole and X means Cl, Br or I, have been investigated by magnetic susceptibility, magnetic saturation and Mössbauer spectroscopy. The experimental temperatures vary from 2 K to room temperature for the magnetic susceptibility measurements and from 4 K to room temperature for the Mössbauer measurements. Mössbauer spectra in an applied magnetic field are also reported. The results of both types of measurements and ligand-field spectra are interpreted using a ligand-field theory. The tetragonal ground-state splitting parameters have been determined using the ligand-field spectra. For the pyrazole compounds, the experimental data nicely agree with theoretical results. The quadrupole splitting and the magnetic properties of these compounds can be completely described within the used model, assuming a tetragonal molecular point symmetry. For the 5-methylpyrazole compounds, the measurements show that the point symmetry is lower than tetragonal. The agreement between the experimental data and the theoretical results for a point group C_i is less fair, especially concerning the V_{zz} and η values. Besides the V_{zz} values of $Fe(mpz)_4X_2$ differ significantly from those of the corresponding $Fe(pz)_4X_2$ compounds.

Introduction

In Part I a ligand-field theory was presented for calculations concerning high spin d^6 ions[1]. Results for both the quadrupole splitting and magnetic susceptibility for powdered compounds, exhibiting particular tetragonal and orthorhombic energy-splitting parameters were mentioned. In the present part the results of magnetic and Mössbauer measurements of series of tetragonal and rhombic Fe(II) compounds are presented. These experimental data are used to test the usefulness and the validity of the theory in Part I.

Experimental Part

Preparation of the Compounds

The preparation of the compounds $Fe(pz)_4X_2$ and $Fe(mpz)_4X_2$ has been mentioned before[2].

Reprint requests to Dr. J. Reedijk, Department of Chemistry, Delft University of Technology, Julianalaan 136, *Delft/Niederlande*.

Mössbauer Spectra

The Mössbauer measurements for the temperature region above 77 K were performed using an Elscint MVT-2 constant acceleration drive with a 400-channel analyzer. Sample temperatures were obtained, using a nitrogen cryostat. The temperature stability was better than 1 K for indefinite periods. Velocity calibration was obtained by the spectrum of a 0.001″ iron foil. The initial intensity of the source was 10 mC ^{75}Co, diffused into 6 μm rhodium foil. The measurements below 77 K were performed by a constant acceleration drive, with the sample in a helium-flow cryostat, or in a helium-bath cryostat. In both cases the temperature accuracy was about 1 K. Concerning the measurements in an applied magnetic field, for both the 4.2 K measurements and the roomtemperature measurements, the direction of the applied magnetic field was parallel to the γ-ray direction. For these measurements, the velocity of the Mössbauer source has been measured simultaneously with the spectra (for the 4.2 K measurements), or afterwards (for the room-temper-

ature measurements), both using a Michelson interferometer.

Magnetic Susceptibility

Magnetization measurements of powdered samples were performed by means of a PAR vibrating sample magnetometer, model 150. For each compound we measured both magnetic saturation from 0 to 52,400 Oersted at distinct temperatures, and magnetic susceptibility in the 2-80 K region with a field of about 5000 Oersted. Magnetic susceptibility measurements above 80 K were performed by a Gouy balance, equipped with a temperature control. This balance has been calibrated with $HgCo(NCS)_4$.

Results and Discussion

General

Previous work[2] presented centre shifts and quadrupole splittings of $Fe(pz)_4X_2$ and $Fe(mpz)_4X_2$ at two distinct temperatures, i.e. at 300 K and 90 K. Now these measurements have been repeated, and performed in the interjacent temperature region and in the temperature region down to 4 K. Moreover, Mössbauer spectra of some compounds have been obtained in an applied magnetic field. The centre shifts and quadrupole splittings at several temperatures are listed in Table 1. It is seen that the quadrupole splitting values of the pyrazole compounds hardly depend on temperature, but that the 5-methylpyrazole compounds exhibit strongly temperature dependent quadrupole splittings. The results for the powder-magnetic moments are shown in Table 2 and those of the magnetic-saturation measurements are listed in Table 3.

Structural Details

In order to explain the experimental results regarding quadrupole splitting, powder-magnetic sus-

Table 1.

Compound	Temperature (K)	δ[a,b]	ΔE_Q[a,b]
$Fe(pz)_4Cl_2$	295	1.32 (1)	0.60 (1)
	221	1.36 (1)	0.59 (1)
	182	1.39 (1)	0.59 (1)
	124	1.42 (1)	0.60 (1)
	86	1.54 (1)	0.59 (1)
	40	1.47 (1)	0.60 (1)
	20	1.49 (1)	0.60 (1)
	4.2	1.48 (1)	0.59 (1)
$Fe(pz)_4Br_2$	295	1.32 (2)	0.55 (2)
	212	1.37 (2)	0.55 (2)
	163	1.40 (2)	0.54 (2)
	82	1.44 (2)	0.54 (2)
	20	1.46 (2)	0.53 (2)
$Fe(pz)_4I_2$	295	1.30 (2)	0.43 (2)
	216	1.36 (1)	0.43 (1)
	154	1.40 (1)	0.44 (1)
	84	1.44 (1)	0.44 (1)
	20	1.47 (1)	0.44 (1)
$Fe(mpz)_4Cl_2$	295	1.33 (1)	1.53 (1)
	259	1.36 (1)	1.63 (1)
	218	1.39 (1)	1.74 (1)
	185	1.41 (1)	1.84 (1)
	165	1.43 (1)	1.91 (1)
	161	1.43 (1)	1.93 (1)
	146	1.44 (1)	1.97 (1)
	134	1.44 (1)	2.00 (1)
	132	1.44 (1)	2.01 (1)
	129	1.45 (1)	2.04 (1)
	125	1.44 (1)	2.06 (1)
	121	1.45 (1)	2.07 (1)
	112	1.45 (1)	2.10 (1)
	98	1.46 (1)	2.14 (1)
	82	1.46 (1)	2.16 (1)
	60	1.47 (1)	2.17 (1)
	40	1.48 (1)	2.18 (1)
	20	1.48 (1)	2.19 (1)
	10	1.48 (1)	2.19 (1)
$Fe(mpz)_4Br_2$	295	1.32 (2)	1.05 (2)
	262	1.34 (2)	1.11 (2)
	215	1.37 (1)	1.20 (1)
	177	1.40 (1)	1.29 (1)
	150	1.42 (1)	1.35 (1)
	122	1.44 (1)	1.42 (1)
	116	1.44 (1)	1.42 (1)
	86	1.45 (1)	1.43 (1)
	60	1.47 (1)	1.44 (1)
	50	1.47 (1)	1.47 (1)
	20	1.47 (1)	1.35 (1)
	10	1.47 (1)	1.35 (1)
$Fe(mpz)_4I_2$	295	1.30 (2)	0.63 (3)
	224	1.34 (1)	0.61 (2)
	215	1.36 (1)	0.61 (2)
	209	1.35 (1)	0.58 (2)
	175	1.38 (1)	0.60 (1)
	139	1.40 (1)	0.60 (1)
	91	1.42 (1)	0.64 (1)
	80	1.44 (1)	0.65 (1)
	60	1.45 (1)	0.65 (1)
	40	1.45 (1)	0.67 (1)
	20	1.46 (1)	0.62 (1)
	10	1.46 (1)	0.62 (1)

The isomer shifts are given with respect to sodium nitroprusside.

[a] Isomer shifts and Quadrupole splittings are in mm/s.

[b] Uncertainties in the last digit are in parentheses.

Table 2.

Compound: $Fe(pz)_4Cl_2$		Compound: $Fe(pz)_4Br_2$		Compound: $Fe(mpz)_4Br_2$		Compound: $Fe(mpz)_4Cl_2$	
Temperature (K)	μ_{powder}[a, b]	Temperature (K)	μ_{powder}[a, b]	Temperature (K)	μ_{powder}[a, b]	Temperature (K)	μ_{powder}[a, b]
2.2	4.87	2.0	4.82	2.1	4.69	115.2	5.48
3.0	4.88	2.9	4.85	3.3	4.77	126.3	5.48
4.7	4.90	4.2	4.91	4.2	4.83	128.6	5.48
9.5	5.05	6.5	5.00	5.6	4.85	131.8	5.49
15.2	5.18	8.6	5.06	8.3	4.97	135.2	5.48
20.8	5.28	14.3	5.19	10.2	5.02	145.1	5.49
24.3	5.36	20.2	5.27	14.7	5.15	162.7	5.48
30.1	5.45	25.1	5.33	18.3	5.21	193.0	5.48
42.0	5.52	30.6	5.38	25.2	5.30	232.4	5.46
55.1	5.55	39.0	5.41	31.6	5.36	263.0	5.46
76.2	5.58	52.3	5.47	39.2	5.41	293.7	5.45
96.0	5.59	65.2	5.50	53.1	5.47		
115.3	5.60	71.0	5.51	70.3	5.50		
144.0	5.59	80.0	5.47	86.2	5.51		
173.2	5.56	83.4	5.50	102.1	5.52		
201.7	5.54	94.2	5.44	138.6	5.52		
232.4	5.53	127.2	5.43	169.3	5.50		
262.0	5.52	197.8	5.42	201.0	5.49		
295.1	5.50	256.0	5.40	254.2	5.46		
		295.0	5.40	294.6	5.46		

[a] μ_{powder} is the powder-magnetic moment in B.M. For low temperatures μ_{powder} has been corrected for saturation effects[3, 4].

[b] The systematic inaccuracy in a whole series of μ values is about 0.05 B.M.; the relative inaccuracy within a series of μ values is about 0.02 B.M.

Table 3. Magnetic-saturation measurements of some Fe(II) compounds

$Fe(pz)_4Cl_2$				$Fe(pz)_4Br_2$	$Fe(mpz)_4Br_2$	
Temperature H[a]	2.0 K M[b]	3.1 K M[b]	4.2 K M[b]	2.1 K M[b]	2.0 K M[b]	4.2 K M[b]
2700	3.85	2.65	1.95	2.95[c]	3.65	1.75
5400	6.90	4.95	4.00	6.70	6.60	3.65
8000	9.15			9.10	9.10	4.95
10600	10.75	8.40	7.15	10.60	10.35	6.30
15700	12.20	10.80	9.50	12.25	12.00	8.60
20800	13.00	12.00		13.10	12.90	10.25
26000	13.40	12.80	12.30	13.60	13.45	11.40
31200	13.70	13.40		13.90	13.80	12.35
36400	13.90	13.80	13.50	14.10	14.10	13.05
41600	14.20	14.10		14.35	14.25	13.60
46800	14.40			14.60	14.50	13.90
52000	14.60	14.60	14.50	14.75	14.70	14.25

[a] H is the magnetic field in Oersted. The uncertainty in H is about 2%.

[b] M stands for the magnetization in units 10^3 · emu/mol. Uncertainties in M are about 1%.

[c] The actual magnetic field strength in this case is 2080 Oersted.

ceptibility and powder-magnetic saturation, structural details are needed on the compounds in study. No crystal structures have been reported, either for the compounds $Fe(pz)_4X_2$, or for $Fe(mpz)_4X_2$. However, crystal structures of $Ni(pz)_4Cl_2$[5], $Ni(pz)_4Br_2$[6], and $Mn(mpz)_4Br_2$[7] have been reported. The X-ray diffraction patterns of the powders of $Ni(pz)_4Cl_2$, $Ni(pz)_4Br_2$ and $Mn(mpz)_4Br_2$ appeared to be very similar in both d values and intensities with those of the corresponding Fe(II) compounds[8]. Therefore the assumption was made that these corresponding Fe(II) compounds have crystal and molecular structures, similar to the Ni(II) and Mn(II) compounds, respectively. The

crystal structures of $Ni(pz)_4Cl_2$ and $Ni(pz)_4Br_2$ are both monoclinic and have space group C2/c with four molecules per unit cell. The only rigorous molecular symmetry element in these molecules is a center of symmetry on the Nickel ion, and thus the rigorous point group is C_i. For the $Ni(N)_4X_2$ unit however, the point symmetry appears to be close to D_{4h}: the Ni-N distances of the two types of different pyrazole rings are nearly the same, and the deviation of the X-Ni-X line with the normal to the plane through the four coordinating nitrogen atoms (the basal plane) is less than 0.5 degrees. For the $Ni(pz)_4X_2$ unit the pyrazole rings are only slightly tilted from a position perpendicular to the basal plane, so that an axis perpendicular to that plane is nearly a fourfold axis, as far as the arrangements of the atoms in the rings are not considered. Since the point symmetry therefore is close to D_{4h}, for the calculation of the paramagnetic behaviour and the quadrupole splitting, the theory as developped in part I[1], can be applied to the compounds $Fe(pz)_4X_2$.

The compound $Mn(mpz)_4Br_2$ has space group $P\bar{1}$ with one molecule per unit cell. The only rigorous element of molecular symmetry is a center of symmetry on the Mn(II) ion, and thus the rigorous point group is C_i. However the point symmetry appears to be close to C_{2h}. As in the two $Ni(pz)_4X_2$ compounds, the Mn-N distances of the two types of different pyrazole rings are nearly the same, and furthermore the deviation of the Br-Mn-Br line from the normal to the plane through the four coordinating nitrogens (the basal plane) is less than 1.5 degrees. Contrary to the pyrazole compounds however, the methylpyrazole rings are tilted much more for a position perpendicular to the basal plane. The values of the tilt angles of the two rings are nearly equal. The consequence of this feature is that, besides the rigorous symmetry element of inversion, the only pseudo-symmetry elements are a twofold axis in the basal plane, and a plane of symmetry, perpendicular to that axis. This results in a point symmetry close to C_{2h}.

Setting up a Hamiltonian for $Fe(mpz)_4Br_2$

Since in Part I[1] the point group D_{2h} is the lowest symmetry that is taken into account, the theory must be adapted to make it suitable to apply to the 5-methylpyrazole compounds in study. The descend in symmetry from D_{4h} to C_{2h} implies that terms have to be added to the crystal-field Hamiltonian:

$$\hat{V}_{\text{c.f.}(C_{2h})} = \hat{V}_{\text{c.f.}(D_{4h})} + \hat{V}_{\text{c.f.}(D_{4h}\to C_{2h})} \cdot \qquad (1)$$

The crystal-field Hamiltonian $\hat{V}_{\text{c.f.}(D_{4h})}$ has been developed in Part I[1]. On symmetry arguments it can be shown that the additional crystalfield Hamiltonian $\hat{V}_{\text{c.f.}(D_{4h}\to C_{2h})}$, written as a linear combination of spherical harmonics, comprises $Y_{2,\pm1}$, $Y_{2,\pm2}$, $Y_{4,\pm1}$, $Y_{4,\pm2}$ and $Y_{4,\pm3}$ as angular dependent operators.

Because there are no longer three orthogonal symmetry axes, the additional terms in the crystal-field Hamiltonian cannot be arranged in Hutchings[9] standard notation $O_n{}^m$. Therefore, the convention will be used, as given by Sugano et al.[10]:

$$\hat{V}_{\text{c.f.}} = \sum_{k=0}^{\infty} \sum_{m=-k}^{k} r^k q_{k,m} C_m{}^k(\theta, \varphi) \qquad (2)$$

in which $q_{k,m}$ are the crystal-depending coefficients of the operator

$$C_{in}{}^k(\theta, \varphi) = \left(\frac{4\pi}{2k+1}\right)^{1/2} Y_{k,m}(\theta, \varphi)$$

that is acting on the angular part of the electronic wavefunctions of the central ion. For deriving expressions for the coefficients $q_{k,m}$ in the crystal-field Hamiltonian, it was assumed that the influence of the 5-methylpyrazole rings on the electrons of the iron ion, can be reflected by three point charges per ring: the coordinating nitrogen and two imaginary charges at some place in the plane of the ring. For C_{2h} point symmetry, the polair coordinates of these twelve point charges are: $(r_1, \theta/2, 0)$, $(r_1, \theta/2, \pi/2)$, $(r_1, \theta/2, \pi)$, $(r_1, \theta/2, 3\pi/2)$ — these are the four coordinating nitrogens —, and $(r_2, \theta_2, \varphi_2)$, $(r_2, \theta_2, \pi/2-\varphi_2)$, $(r_2, \pi-\theta_2, \pi+\varphi_2)$, $(r_2, \pi-\theta_2, 3\pi/2-\varphi_2)$, $(r_3, \theta_3, \varphi_3)$, $(r_3, \theta_3, \pi/2-\varphi_3)$, $(r_3, \pi-\theta_3, \pi+\varphi_3)$, and $(r_3, \pi-\theta_3, 3\pi/2-\varphi_3)$. The coefficients $q_{k,m}$ are complex numbers. For small θ_2, θ_3, φ_2, and φ_3, it can be shown that $q_{2,1}$ and $q_{4,1}$ are proportional to $(1-i)$, $q_{4,3}$ is proportional to $(1+i)$ and q_{22} and $q_{4,2}$ are purely imaginary. Furthermore, in this case, the following relations between the coefficients can be drawn:

$$\frac{q_{4,1}}{q_{2,1}} = (1.5\sqrt{2})\frac{q_{4,2}}{q_{2,2}} \qquad (4)$$

and

$$\frac{q_{4,1}}{q_{4,3}} = (-3/\sqrt{7})\frac{1-i}{1+i} \qquad (5)$$

and besides $q_{2,2}$ has a sign opposite to $q_{4,2}$. Evaluating the radial parts of the matrix elements, a crystal-field Hamiltonian can be obtained that is acting on the angular parts of the wavefunctions:

$$\hat{V}'_{\text{c.f.}(C_{2h})} = \hat{V}'_{\text{c.f.}(D_{4h})} + 7\,(Q_{2,1}\,C^2_1 + Q_{2,-1}\,C^2_{-1} + Q_{2,2}\,C^2_2 + Q_{2,-2}\,C^2_{-2}) + 21\,(Q_{4,1}\,C^4_1 + Q_{4,-1}\,C^4_{-1} + Q_{4,2}\,C^4_2 + Q_{4,-2}\,C^4_{-2} + Q_{4,3}\,C^4_3 + Q_{4,-3}\,C^4_{-3}) \quad (6)$$

where

$$Q_{2,m} = \frac{1}{7} \cdot \int r^2\, R_{3d}(r)\, q_{2,m}\, R_{3d}(r)\, r^2\, \mathrm{d}r \quad (7)$$

and

$$Q_{4,m} = \frac{1}{21} \cdot \int r^4\, R_{3d}(r)\, q_{4,m}\, R_{3d}(r)\, r^2\, \mathrm{d}r \quad (8)$$

in which $R_{3d}(r)$ stands for the radial part of the electronic $3d$ wavefunction. It holds that

$$Q_{k,-m} = (Q_{k,m})^*\,(-1)^m\,. \quad (9)$$

In descending the point symmetry from D_{4h} to C_{2h}, the following additional matrix elements appear in the energy matrix $\langle L_z, S_z|\ \hat{V}'_{\text{c.f.}}\ |L_z', S_z'\rangle$:

$$\langle 2, S_z|\ \hat{V}'_{\text{c.f.}}\ |1, S_z'\rangle = \delta_{S_z,S_z'}\,(\sqrt{6}\,Q_{2,1} - \sqrt{5}\,Q_{4,1})\,, \quad (10)$$

$$\langle 1, S_z|\ \hat{V}'_{\text{c.f.}}\ |0, S_z'\rangle = \delta_{S_z,S_z'}\,(Q_{2,1} + \sqrt{30}\,Q_{4,1})\,, \quad (11)$$

$$\langle 2, S_z|\ \hat{V}'_{\text{c.f.}}\ |-1, S_z'\rangle = \delta_{S_z,S_z'}\,(-\sqrt{35}\,Q_{43})\,, \quad (12)$$

$$\langle 1, S_z|\ \hat{V}'_{\text{c.f.}}\ |-1, S_z'\rangle = \delta_{S_z,S_z'}\,(-\sqrt{6}\,Q_{2,2} - 2\sqrt{10}\,Q_{4,2})\,, \quad (13)$$

and

$$\langle 2, S_z|\ \hat{V}'_{\text{c.f.}}\ |0, S_z'\rangle = \delta_{S_z,S_z'}\,(-2\,Q_{2,2} + \sqrt{15}\,Q_{4,2})\,, \quad (14)$$

and all other additional matrix elements that appear by changing the signs of L_z and L_z' in expressions (10) to (14). These other additional matrix elements can be calculated, using (9) to (14). For the mpz compounds in study it was assumed that the values of θ_2, θ_3, φ_2, and φ_3 are small. Then, real energy parameters $V_{k,m}$ can be introduced, by making the following substitutions:

$$V_{2,2} = Q_{2,2}/i\,, \quad (15)$$

$$V_{4,2} = Q_{4,2}/i\,, \quad (16)$$

$$V_{2,1} = Q_{2,1}/(1+i)\,, \quad (17)$$

$$V_{4,1} = Q_{4,1}/(1-i)\,, \quad (18)$$

and

$$V_{4,3} = Q_{4,3}/(1+i)\,. \quad (19)$$

After diagonalizing the energy matrix, the paramagnetic behaviour and the valence contribution to the EFG tensor was calculated in a way, analogous to that in Part I[1]. The lattice contribution to the EFG tensor was found from the relation that exists between the second order crystal-field parameters and the lattice contribution to the EFG tensor. The three additional terms of the lattice contribution to the EFG tensor are:

$$\tfrac{1}{2}\,e\,Q\,V_{xy,\text{lat}} = -1.148\,V_{2,2}/10^3\ \text{mm/s}\,, \quad (20)$$

$$\tfrac{1}{2}\,e\,Q\,V_{xz,\text{lat}} = -1.148\,V_{2,1}/10^3\ \text{mm/s}\,, \quad (21)$$

$$\tfrac{1}{2}\,e\,Q\,V_{yz,\text{lat}} = +1.148\,V_{2,1}/10^3\ \text{mm/s} \quad (22)$$

in which the energy parameters $V_{2,2}$ and $V_{2,1}$ are expressed in cm^{-1}.

Furthermore, $\eta_{\text{lat}} = 0$. This is easily seen from symmetry arguments, because $x^2 - y^2$ is a basis of the irreducible representation B_{2g} in the point-group C_{2h}.

Fits and Evaluation of the Theory

As shown in Part I[1], the quadrupole splitting and magnetic susceptibility behaviour can be calculated when the spectrochemical parameters, the spin-orbit coupling parameter and the orbital-reduction factor are known. This means that from estimates of these parameters a calculated curve may be drawn.

The pyrazole compounds:

For the compounds $Fe(pz)_4X_2$ of nearly tetragonal structure, we need to know three spectrochemical parameters: Dq^{xy}, Ds and Dt. The ligand-field spectra only yield two bands[2]. For determining Dq^{xy}, Ds and Dt, the assumption was made that the proportion Ds/Dt in these Fe(II) compounds is equal to that in the corresponding Ni(II) compounds[11,12]. For the spin-orbit coupling parameters, two parameters $\lambda_{||}$ and $\lambda_{\perp}$ were taken into account, as in the case of the corresponding Ni(II) compounds[11]. It was assumed that the proportional reductions of these spin-orbit coupling parameters with respect to the free ion value are, in the case of the compounds $Fe(pz)_4X_2$, the same as in the cor-

responding Ni(II) compounds[11,12]. The resulting values for $\lambda_{||}$ and $\lambda_{\perp}$, and the spectrochemical parameters are shown in Table 4. The Dq^{xy} values of the three compounds appear to be close together, and also near the value $Dq = 1100\ cm^{-1}$ for the compound $Fe(pz)_6(BF_4)_2$[13,14], Using the calculated parameters for the three compounds $Fe(pz)_4X_2$, the resulting quadrupole splittings are hardly dependent on temperature in the relevant temperature region below 300 K. The experimental quadrupole splittings also appeared to be temperature independent, within the experimental error. A comparison of the calculated and the experimental quadrupole splitting is shown in Table 5. The sign of the quadrupole splitting of $Fe(pz)_4Cl_2$ was determined by measuring a Mössbauer spectrum at 4.2 K in an applied magnetic field of 10.4 kOe. This spectrum is shown in Figure 1.

The spectrum can be understood as arising from a compound with a small internal magnetic field, induced by the applied magnetic field of 10.4 kOe. Since the internal magnetic field is expected to be along the speudo-tetragonal axis (since the g values of the lowest energy levels ca are calculated as[1] $g_{||} \approx 10$ and $g_{\perp} \approx 0$), the only way in which the spectrum can be explained is when V_{zz} is negative. Thus for $Fe(pz)_4Cl_2$ the calculated sign of V_{zz}, and the course of the quadrupole-splitting curve is in agreement with the experimental data. Regarding the value of the quadrupole splitting, there is no complete agreement between theory and experiment. Noting this, it is necessary to remark that the quadrupole splitting is the result of two contributions that are opposite in sign, and that therefore the difference between theory and experiment must be compared with the whole range of possible quadrupole splittings for high-spin Fe(II) compounds, covering over 4 mm/s.

For the other two pyrazole compounds in study, $Fe(pz)_4Br_2$ and $Fe(pz)_4I_2$, it is assumed that they have likewise a negative sign of V_{zz}. This equality in sign is based on the resemblance in structural and spectrochemical properties. A comparison between theoretical and experimental results learns that for these two compounds there is a better agreement for the numerical quadrupole-splitting value, than in the case of $Fe(pz)_4Cl_2$.

The small temperature dependence of the quadrupole splitting of the three compounds indicates that the deviation from tetragonal symmetry must be very small. For example, an orthorhombic distortion, such that $Du + Dv > 10\ cm^{-1}$ [1], would influence the valence contribution to the quadrupole splitting such that an experimentally detectable

Table 4. Spectro chemical and spin-orbit coupling parameters of $Fe(pz)_4X_2$ for two temperatures. Parameters in cm^{-1}.

Compound	Dq^{xy}		Ds		Dt		$\lambda_{||}$	$\lambda_{\perp}$
	295 K	90 K	295 K	90 K	295 K	90 K		
$Fe(pz)_4Cl_2$	1060	1160	1025	1060	280	290	− 80	−85
$Fe(pz)_4Br_2$	1020	1100	1210	1230	335	335	− 90	−85
$Fe(pz)_4I_2$	1070	1090	1460	1510	460	480	−105	−85

Table 5. Comparison of calculated and experimental quadrupole splittings for $Fe(pz)_4X_2$ at temperatures 295 K and 90 K respectively. Quadrupole splittings in mm/s.

Compound	Temperature 295 K				Temperature 90 K			
	calculated			exp.	calculated			exp.
	$\Delta E_{Q_{val}}$[a]	$\Delta E_{Q_{lat}}$[b]	ΔE_Q	$\lvert\Delta E_Q\rvert$[c]	$\Delta E_{Q_{val}}$	$\Delta E_{Q_{lat}}$	ΔE_Q	$\lvert\Delta E_Q\rvert$
$Fe(pz)_4Cl_2$	−1.87	0.97	−0.90	0.60	−1.87	1.00	−0.87	0.59
$Fe(pz)_4Br_2$	−1.88	1.16	−0.72	0.55	−1.88	1.18	−0.70	0.54
$Fe(pz)_4I_2$	−1.88	1.40	−0.48	0.43	−1.88	1.44	−0.44	0.44

[a] Calculated valence contribution to the quadrupole splitting.
[b] Calculated lattice contribution to the quadrupole splitting.
[c] Absolute value of the experimental quadrupole splitting.

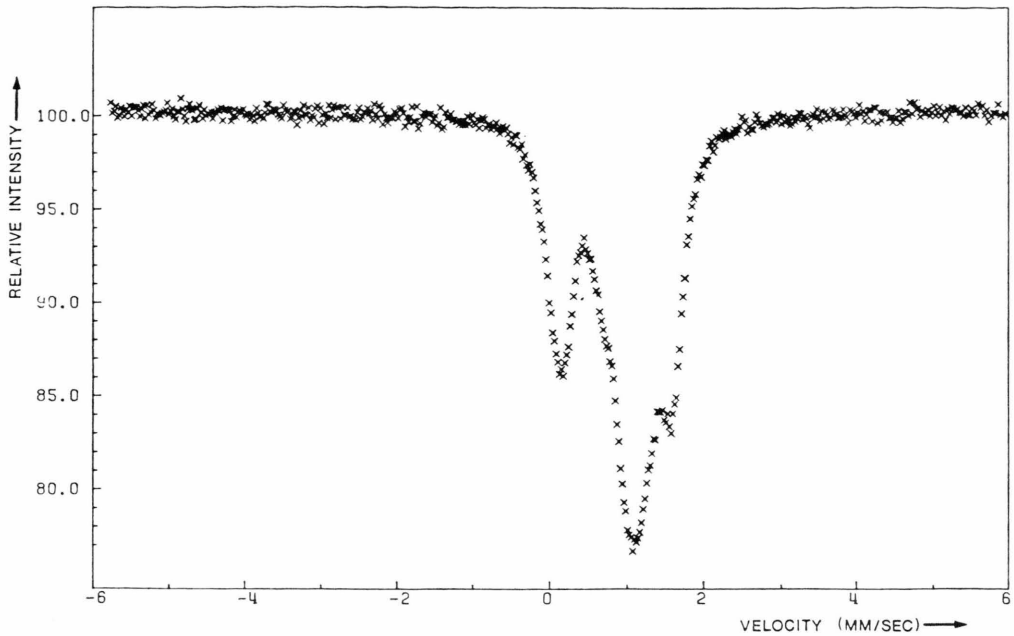

Fig. 1. Mössbauer spectrum of $Fe(pz)_4Cl_2$ at 4.2 K in an applied magnetic field of 10.4 kOe.

maximum in the curve of the quadrupole splitting versus temperature would be found.

The calculated curves of experimental powder-magnetic moments for $Fe(pz)_4Cl_2$ and $Fe(pz)_4Br_2$ are shown in Fig. 2 and 3. The values of the orbital-reduction factor k, that give the best fit, are 1.0 for $Fe(pz)_4Cl_2$ and 0.9 for $Fe(pz)_4Br_2$.

For $Fe(pz)_4Cl_2$ the largest deviations between the theoretical curve and the experimental measurements are found at very low temperatures. For $Fe(pz)_4Br_2$ the deviations between the theoretical curve and the experimental data do not exceed 0.10 B.M. for any temperature. In the 10—80 K region the experimental values of μ_{powder} are systematically higher than theory predicts, in the 100—200 K region, the experimental values are lower. The discontinuity in the experimental μ_{powder} values of $Fe(pz)_4Br_2$ at about 85 K coincides with the temperature where the measuring method was changed: the powder-magnetic moments at 83.4 K, 71.0 K and underneath were obtained by a PAR vibrating sample magnetometer, the powder-magnetic moments at 80.0 K, at 94.2 K and above were obtained by a Gouy balance. Therefore, we assume

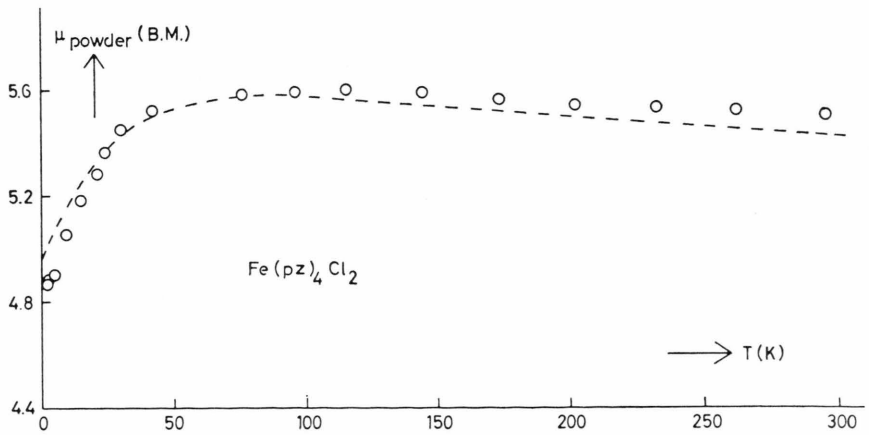

Fig. 2. Calculated curve of the powder paramagnetic moment for $Dq = 1160\ cm^{-1}$, $Ds = 1060\ cm^{-1}$, $Dt = 290\ cm^{-1}$, $\lambda_{\parallel} = -80\ cm^{-1}$, $\lambda_{\perp} = -85\ cm^{-1}$ and $k = 1.0$. Measurements for $Fe(pz)_4Cl_2$ are shown as circles.

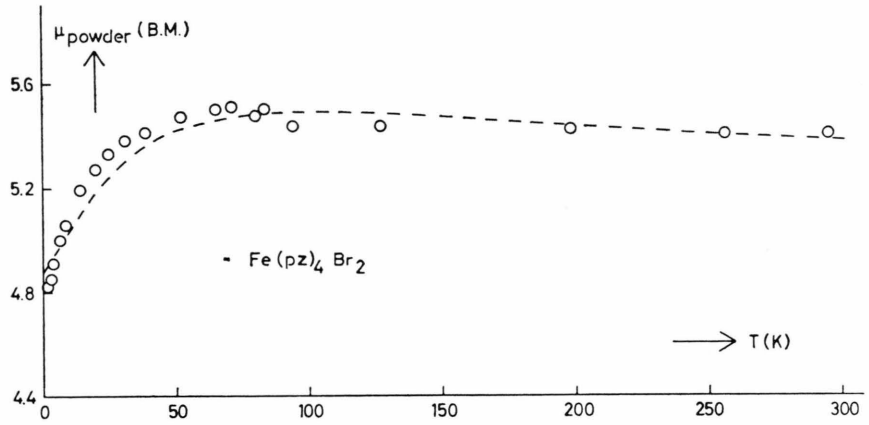

Fig. 3. Calculated curve of the powder paramagnetic moment for $Dq = 1100$ cm^{-1}, $Ds = 1230$ cm^{-1}, $Dt = 335$ cm^{-1}, $\lambda_{\parallel} = -90$ cm^{-1}, $\lambda_{\perp} = -85$ cm^{-1} and $k = 0.9$. Measurements for $Fe(pz)_4Br_2$ are shown as circles.

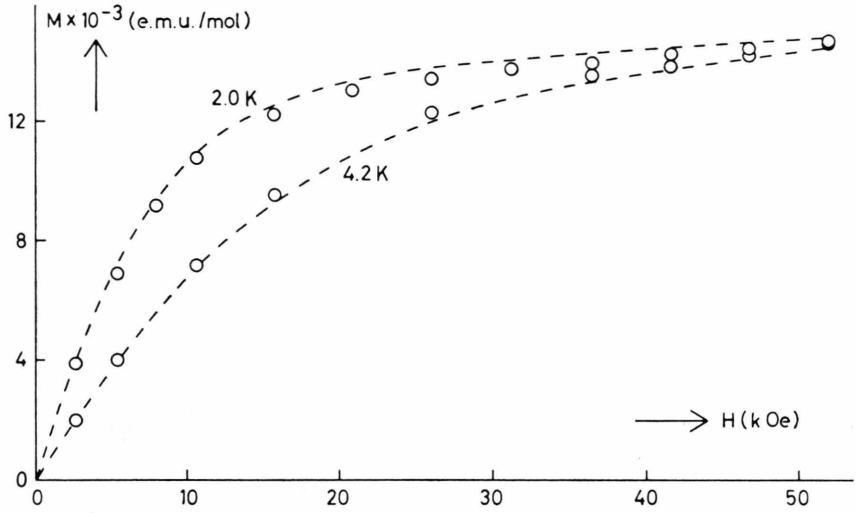

Fig. 4. Calculated magnetization curves for the temperatures 2.0 and 4.2 K. Energy parameters as in Figure 2. Measurements for $Fe(pz)_4Cl_2$ are shown as circles.

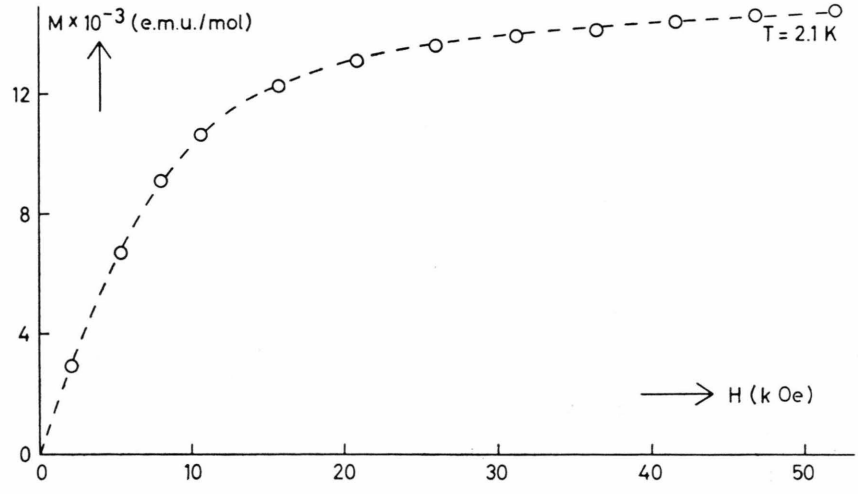

Fig. 5. Calculated magnetization curve for the temperature 2.1 K. Energy parameters as in Figure 3. Measurements for $Fe(pz)_4Br_2$ are shown as circles.

that this discontinuity does not reflect physical phenomena, but reflects a change in experimental circumstances.

The calculated magnetic saturation curves and the experimental data are shown in Fig. 4 and 5. The calculation of the theoretical curves has been performed as denoted in Part I[1]. For $Fe(pz)_4Br_2$ there is a fair fit, as well as for $Fe(pz)_4Cl_2$ at 4.2 K. For $Fe(pz)_4Cl_2$ at 2.0 K the agreement is poorer; the experimental magnetizations are systematically lower than the calculated ones.

In addition it was tried to determine the magnetic behaviour of the lowest energy level by EPR spectroscopy at liquid hydrogen temperature. Unfortunately no clear signals could be observed.

The 5-methyl pyrazole compounds:

The quadrupole-splitting values of the mpz compounds are considerably higher than those of the pz compounds, whereas the *Ds* and *Dt* values in the corresponding compounds are of the same order of magnitude. This difference in magnitude and in temperature dependence is apparently a manifestation of the fact that the symmetry is lower than tetragonal.

Only for $Fe(mpz)_4Br_2$ sufficient structural information is known to set up calculations of the quadrupole splitting and the powder-magnetic moment. As demonstrated before, the structure is such that the point group is close to C_{2h}.

Results of the Mössbauer spectra of $Fe(mpz)_4Br_2$ in the 10—295 K region are listed in Table 1. Besides Mössbauer spectra were recorded at 4.2 K without and with an applied magnetic field. These spectra are shown in Figure 6.

For an applied magnetic field of 10.4 kOe a Mössbauer spectrum was obtained that closely resembles a Mössbauer spectrum of a compound with a quadrupole doublet and an internal magnetic field. Obviously, the applied magnetic field induces an internal magnetic field that is, for most crystallites in the polycrystalline sample, directed in the same direction with respect to the molecular axes. This feature can be understood, because the paramagnetic g values of the lowest two energy levels are strongly anisotropic, i.e. $g_{||} \approx 10$ and $g_{\perp} \approx 0$. Therefore, an applied magnetic field will induce an internal magnetization along this pseudo-tetragonal molecular axis. Because this induced magnetic field appears to be much larger than the external mag-

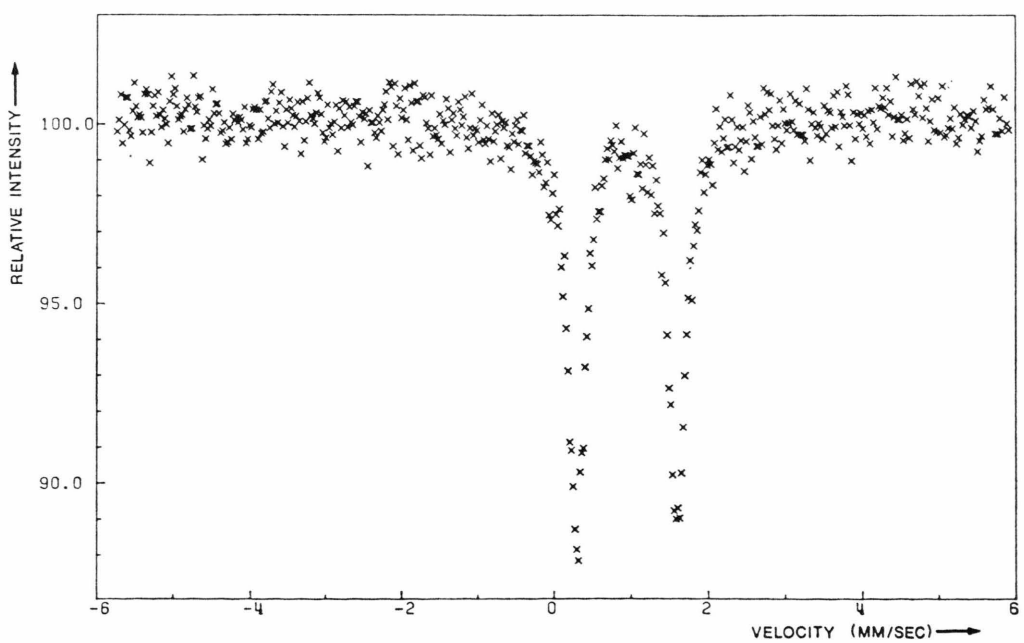

Figure 6 a

Fig. 6. Mössbauer spectra of $Fe(mpz)_4Br_2$ at 4.2 K. a) Without external magnetic field. b) In an applied magnetic field of 10.4 kOe. c) In an applied magnetic field of 47.0 kOe.

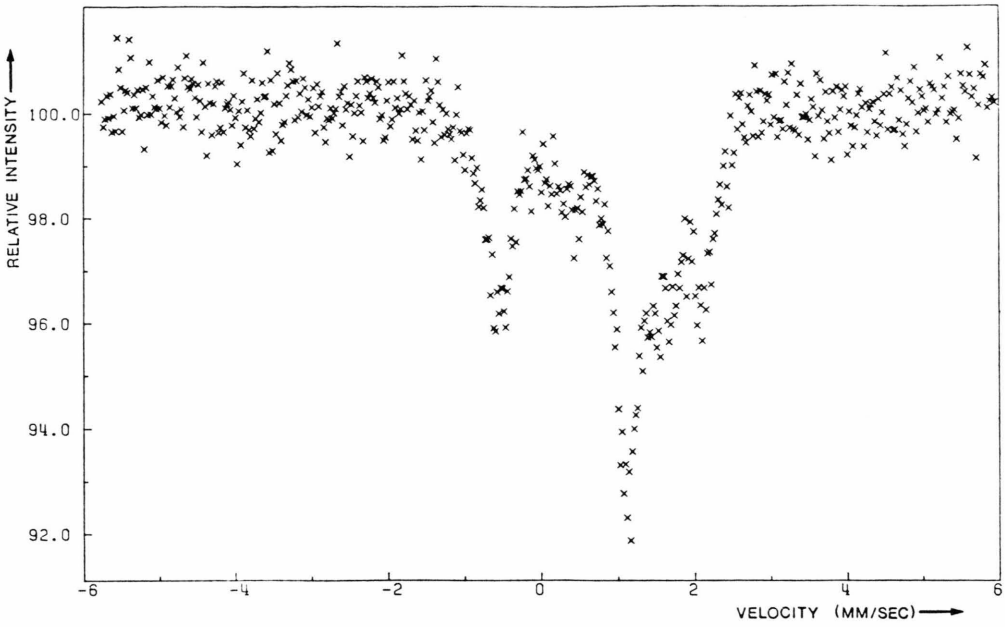

Figure 6b

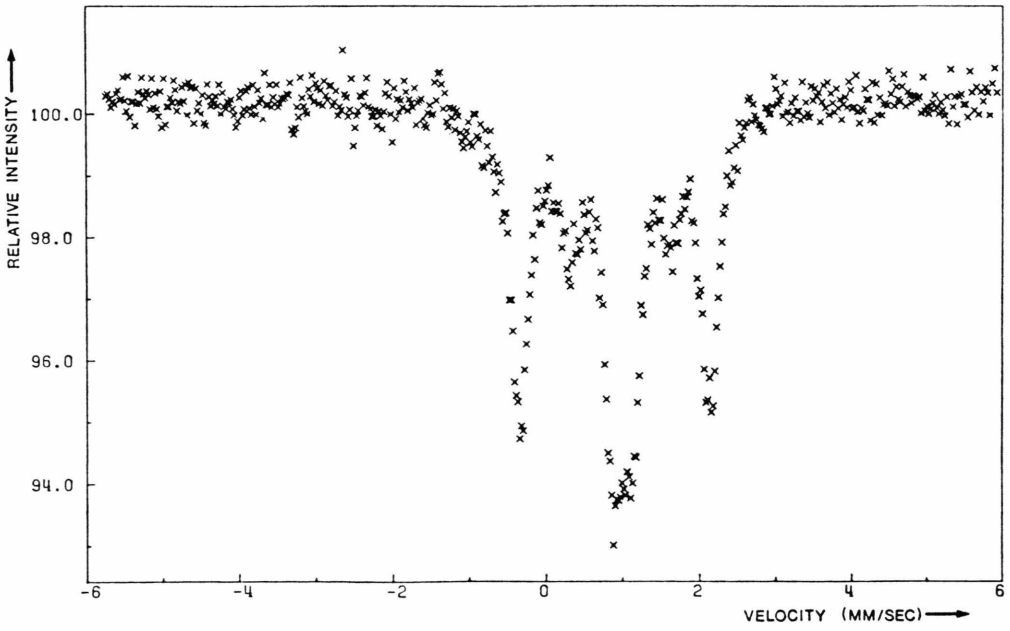

Figure 6c

netic field of 10.4 kOe, the direction of the total magnetic field at the iron nucleus will be close to the direction of the principal molecular axis. Thus, the Mössbauer spectrum at an applied magnetic field of 10.4 kOe can be interpreted as an eight line spectrum with two additional peaks at the positions of the quadrupole doublet without an applied magnetic field. (These two remaining lines are caused by those crystallites, where the external magnetic field is perpendicular to the pseudo-tetragonal axis, so that no magnetic field is induced.)

The eight-line spectrum, however, could not be fitted with a least square fit of eight lorentz lines. Apparently the applied magnetic field, that is randomly orientated with respect to the molecular axes influences the Mössbauer lines too much to be Lorentzian in this case. Therefore, the positions of the eight lines had to be estimated from the spectrum. This is shown in Figure 7.

With these eight line positions Mössbauer parameters were calculated. The best fit was calculated by using a computer program, given by Van Dongen Torman et al.[16]. This fit implies: $\Delta E_Q = -1.35$ mm/s, $\delta = 0.98$ mm/s with respect to the ^{57}Co/Rh source, and an internal magnetic field $H = 60$ kGauss. The good agreement with these parameters concerns peak positions as well as intensities.

As stated before[16], there is no unique solution for V_{zz}, η, and the angles between the internal magnetic field and the principal axis of the EFG tensor. Instead there is a range of possible solutions. For this Mössbauer spectrum of $Fe(mpz)_4Br_2$, there is a range of possible solutions between the extreme $e\,Q\,V_{zz}/2 = -1.32$ mm/s, $\eta = 0.38$ and polair angles between the magnetic field and the EFG tensor: $\theta = 18.5°$, $\varphi = 0°$ and the extreme $e\,Q\,V_{zz}/2 = -1.26$ mm/s, $\eta = 0.66$ and polair angles $\theta = 14.1°$, $\varphi = 90°$.

The possible θ angles are small and thus in very good agreement with the earlier assumption that the direction of the total magnetic field is mainly determined by the induced magnetic field, which is parallel to the pseudo-tetragonal axis of the molecule.

In this case in studying the quadrupole-splitting behaviour and the magnetic properties of $Fe(mpz)_4Br_2$ there is no possibility of a pure evaluation of the validity of the theory set up before[1], because some energy parameters are unknown. It was stated before that in descending point symmetry from D_{4h} to C_{2h} three additional independent energy parameters must be involved in the calculations. The values of these energy parameters are not known, because they cannot be determined from ligand-field reflectance spectra. So the study of the quadru-

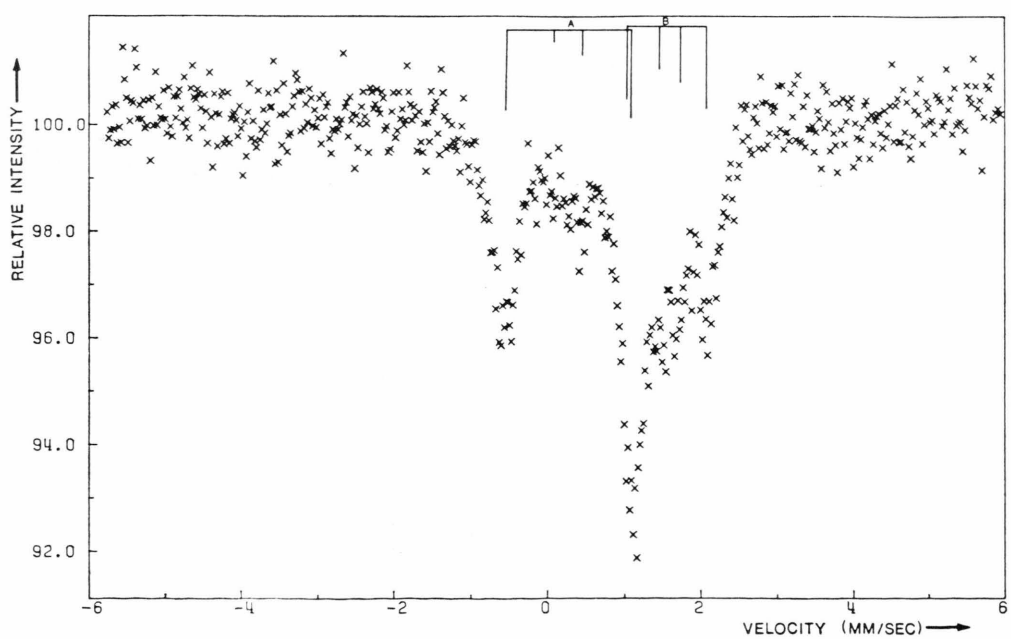

Fig. 7. Assignment of the lines in the Mössbauer spectrum of $Fe(mpz)_4Br_2$ in an applied magnetic field of 10.4 kOe. The four lines originating from the lower quadrupole excited-state levels are denoted by A and those originating from the higher quadrupole excited-state levels by B.

pole-splitting and the magnetic properties of $Fe(mpz)_4Br_2$ has necessarily to be a mixture of an evaluation of the theory and a determination of energy parameters.

Trying to fit the course of the quadrupole-splitting curve by introducing trial values for the three additional energy parameters V_{22}, V_{42} and V_{21}, it appears to be that there is no set at all of V_{22}, V_{42} and V_{21} by which the quadrupole-splitting curve can be fitted. This is due to the fact that for imaginary Q_{22} and Q_{42} and complex Q_{21} the calculated quadrupole-splitting versus temperature is a constantly decreasing curve when temperature increases. The course of the calculated quadrupole-splitting curve is mainly determined by the contribution of the sixth $3d$ electron of the Fe(II) ion. Because we have very less doubt about this part of the theory it seems inevitable to admit that a lowering of the assumed point symmetry C_{2h} is necessary to describe the quadrupole-splitting behaviour adequately. According to the real point symmetry C_i this implies the addition of Q'_{22} and Q'_{42} that both have real values. In Fig. 8 the calculated quadrupole-splitting curve and the curve of the powder-paramagnetic moment has been shown as well as the experimental data. The correspondence between the calculated and the experimental values of the quadrupole splitting is fair, although the fit is not unique; other sets of energy parameters V_{22}, V_{42}, V_{21}, V'_{22} and V'_{42} also deliver a fair fit. All these possible sets deliver the same calculated V_{zz} and η values at 4 K: $e\,Q\,V_{zz} = -0.70$ mm/s and $\eta = 3.06$. These values of V_{zz} and η differ considerably from the experimentally determined ones by the measurements in an applied magnetic field: experimentally has been found $e\,Q\,V_{zz}/2$ is between -1.32 and -1.26 mm/s and η ranges from 0.38 to 0.66.

From our theoretical considerations it was deduced that V_{zz} has about the same size for the compounds $Fe(pz)_4Br_2$ and $Fe(mpz)_4Br_2$, because their Ds and Dt values are close together and V_{xz} and V_{yz} for $Fe(mpz)_4Br_2$ are small. Apparently this is not true. This difference in V_{zz} must be due to some aspect ignored in our theory[1].

A similar deviating behaviour was found for $Fe(mpz)_4Cl_2$ with respect to $Fe(pz)_4Cl_2$: the value of $e\,Q\,V_{zz}/2$ is considerably different in these two compounds, because $e\,Q\,V_{zz}/2$ for $Fe(mpz)_4Cl_2$ could definitely be determined as negative. This sign has been determined by measuring the room-temperature Mössbauer spectrum of $Fe(mpz)_4Cl_2$ in an applied magnetic field of 17.5 kOe. The resulting spectra are shown in Figure 9.

A least-square fit based on a double and a triple line as given by Collins[15] shows positively that the most broadening line, the doublet, is at lower velocity and thus $eQ\,V_{zz}/2$ is negative. This means that for $Fe(mpz)_4Cl_2$ that exhibits a quadrupole splitting of 1.53 mm/s at room temperature, the value $|eQ\,V_{zz}/2|$ must be considerably larger than the value of 0.60 mm/s measured for $Fe(pz)_4Cl_2$.

Obviously in the theoretical model[1] an aspect has been neglected that appears to be important for the

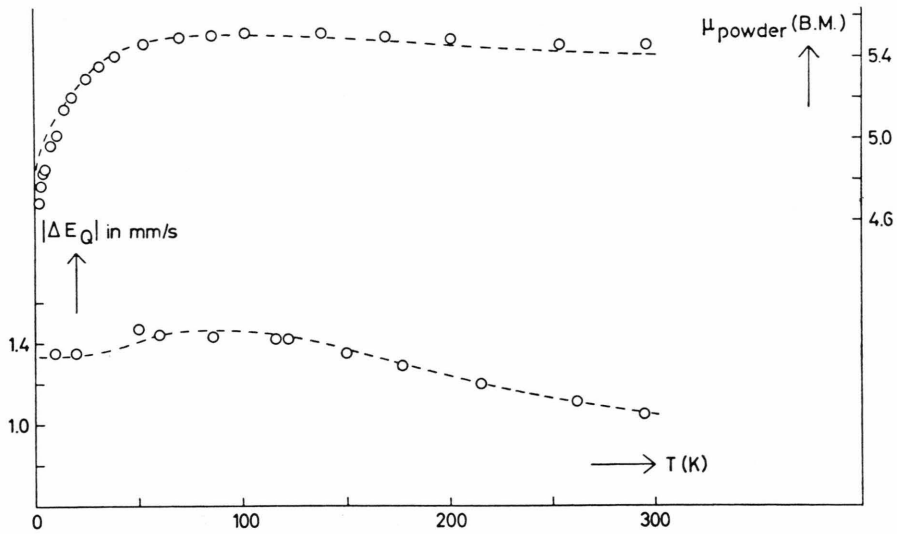

Fig. 8. Calculated curves of quadrupole splittings and powder paramagnetic moments for
$Dq = 1090$ cm^{-1},
$Ds = 1250$ cm^{-1},
$Dt = 300$ cm^{-1},
$Du = 100$ cm^{-1},
$Dv = -48$ cm^{-1},
$V_{22} = -100$ cm^{-1},
$V_{42} = 25$ cm^{-1},
$V_{21} = -200$ cm^{-1},
$\lambda_{\parallel} = -85$ cm^{-1},
$\lambda_{\perp} = -80$ cm^{-1}
and $k = 1.0$. Measurements for $Fe(mpz)_4Br_2$ are shown as circles.

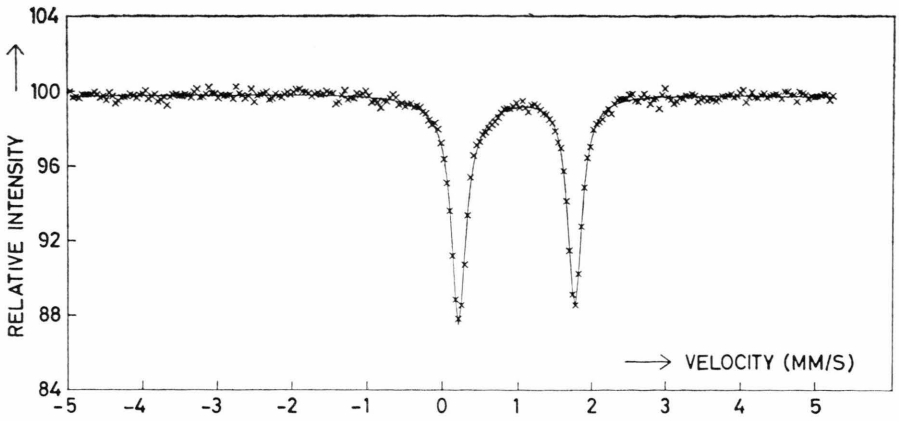

Fig. 9. Mössbauer spectra of $Fe(mpz)_4Cl_2$ at room temperature.

a) Without external magnetic field.

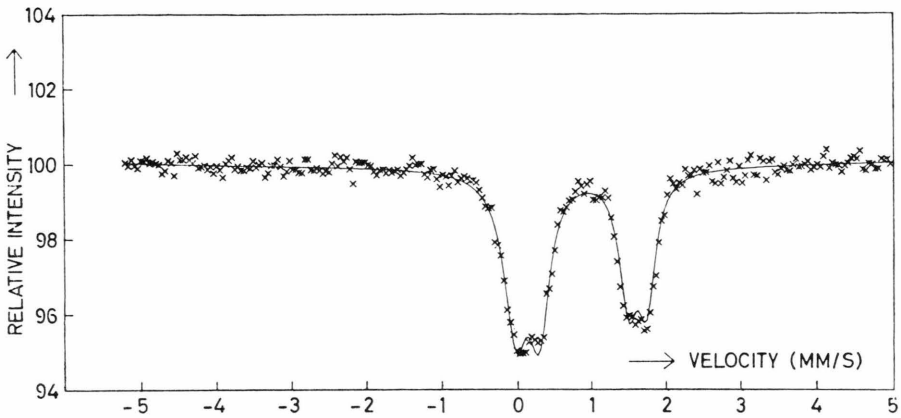

b) In an applied magnetic field of 17.5 kOe.

magnitude of the quadrupole splitting of the mpz compounds. It is not quite clear which of our assumptions in the theoretical model is mainly responsible for the inadequacy of the theory with respect to $Fe(mpz)_4Cl_2$ and $Fe(mpz)_4Br_2$.

A possible explanation might be that electron donation is incorrectly ignored in the theory if it is applied to the 5-methyl pyrazole compounds. Electron donation by π-interaction between the $3d_{zx}$ and $3d_{yz}$ orbitals and the π-electrons of the 5-methyl pyrazole rings may be important in the mpz compounds, because of the tilt of the rings from their perpendicular positions thus approaching the d_{zx} and d_{yz} orbitals of Fe(II). The tilt angle is not close to 45° indeed, which is the ideal tilt angle for π-interaction and which has been found for the compound $Fe(py)_4Cl_2$[17], but the actual tilt angle of mpz might still be important.

Concerning the magnetic measurements the best fit to be obtained for $Fe(mpz)_4Br_2$ is shown in Figure 8. A set of parameters with a better agreement in the low-temperature region yields a larger deviation for higher temperatures. Just like the experimental powder-paramagnetic moments are lower than the calculated values at very low temperatures, the experimental magnetic saturation data are lower than the calculated ones as shown in Figure 10.

A Special Feature in the Quadrupole-Splitting Behaviour of $Fe(mpz)_4Cl_2$

A curve of the experimental quadrupole splitting of $Fe(mpz)_4Cl_2$ is shown in Figure 11. The smooth curve exhibits an irregularity at about 130 K. Around this temperature the quadrupole-splitting curve is steeper. Besides the two Mössbauer spectrum lines have been broadened at this temperature as shown in Table 6. These two phenomena indicate that there is a phase transition of the compounds at about 130 K. An effect of hysteresis could not be detected. The temperature dependence of the ligand-field spectra[12] showed no irregularity around 130 K

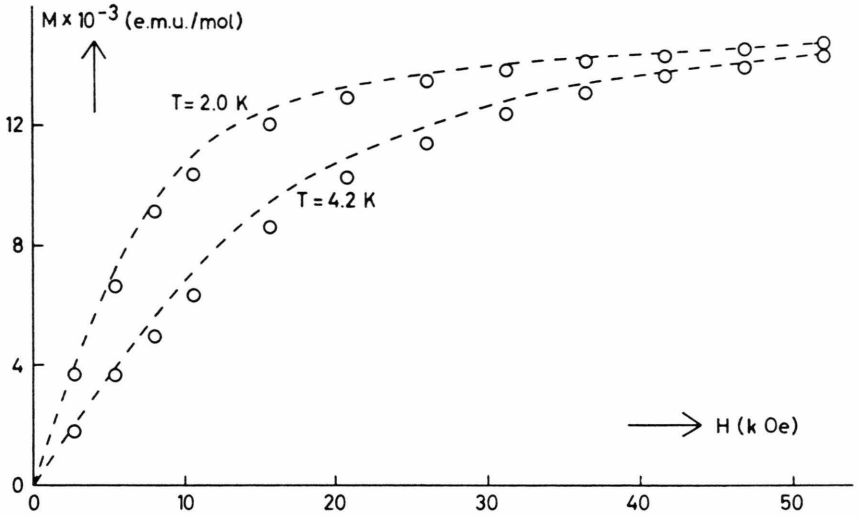

Fig. 10. Calculated magnetization curves for the temperatures 2.0 and 4.2 K. Energy parameters as in Figure 9.

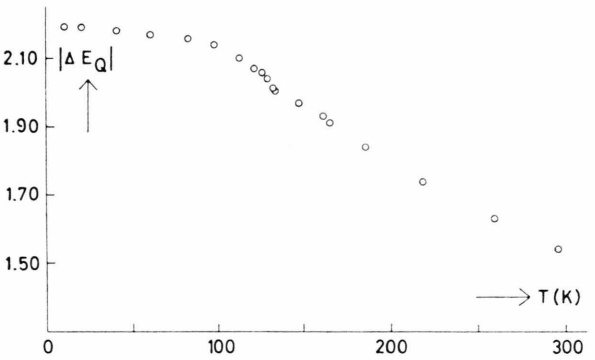

Fig. 11. Experimental quadrupole-splitting data versus temperature for the compound $Fe(mpz)_4Cl_2$.

Table 6. Mössbauer data of $Fe(mpz)_4Cl_2$ near the temperature of its structural phase transition.

T (K)[a]	ΔE_q[b]	Γ_1[c]	Γ_2[c]
134	1.99	0.30	0.27
132	2.01	0.31	0.27
129	2.04	0.40	0.34
125	2.06	0.37	0.34
112	2.10	0.36	0.33
98	2.14	0.29	0.29

[a] Temperature in degrees Kelvin.

[b] Quadrupole splitting in mm/s. The uncertainty is about 0.01 mm/s.

[c] Line width of the two Mössbauer lines in mm/s. The uncertainty is about 0.01 mm/s. Γ_1 concerns the line, lowest in Mössbauer velocity.

and as shown in Table I, the powder-magnetic moment shows not a sudden change at this temperature. Therefore it can be concluded that the concerning phase transition cannot involve a drastical change of the molecular structure with respect to the coordination of the Fe(II) ion.

Conclusions

1. For the compounds $Fe(pz)_4X_2$ there is a fair agreement between experimental magnetic and quadrupole-splitting measurements and their values calculated in a crystal-field model. The lattice contribution to the EFG calculated in this crystal-field model appeared to be relatively reliable for these compounds.
2. The assumed point symmetry D_{4h} for the compounds $Fe(pz)_4X_2$ is in very good agreement with the small temperature dependence of the quadrupole splittings.
3. The agreement for $Fe(mpz)_4Br_2$ and $Fe(mpz)_4Cl_2$ is much lass fair than for the pyrazole compounds.
4. For the compound $Fe(mpz)_4Br_2$ point symmetry C_i must be assumed to explain the course of the quadrupole-splitting curve.
5. The value $eQ\,V_{zz}/2$ for $Fe(pz)_4Cl_2$ and $Fe(pz)_4Br_2$ is strongly different from that of $Fe(mpz)_4Cl_2$ and $Fe(mpz)_4Br_2$ respectively.
6. The compound $Fe(mpz)_4Cl_2$ exhibits a phase transition at about 130 K which is observed only with Mössbauer spectroscopy.

Acknowledgements

The authors are indebted to Dr. G. Lodder for the availability of a multi-channel analyzer, to Drs. S. J. H. Ferrier for his assistance concerning electronical problems and Mr. J. A. Smit for the preparation of some of the compounds. The authors are furthermore greatly indebted to Drs. H. Th. Le Fever and J. J. M. Steijger (Kamerlingh Onnes Laboratory, Leiden) for carrying out Mössbauer measurements in a magnetic field at room temperature, to Dr. J. M. Trooster (Catholic University of Nijmegen) for carrying out Mössbauer measurements in a magnetic field at 4.2 K and for his helpful discussion in interpreting these spectra and to Dr. A. M. van der Kraan (Inter University Reactor Institute, Delft) for carrying out Mössbauer measurements in the 5—80 K temperature range. Drs. H. T. Witteveen, M. C. Cadee and D. W. Engelfriet are gratefully thanked for carrying out the magnetic measurements in the 2—80 K temperature range. Prof. Dr. E. König (Erlangen) is thanked for critically reading the manuscripts.

[1] A. Vermaas, W. L. Groeneveld, and J. Reedijk, Part I.
[2] J. Reedijk and D. W. Engelfriet, Rec. Trav. Chim. **91**, previous paper 883 [1972].
[3] V. R. Marathe and S. Mitra, Chem. Phys. Letters **27**, 103 [1974].
[4] A. Vermaas and W. L. Groeneveld, Chem. Phys. Letters **27**, 583 [1974].
[5] C. W. Reimann, A. D. Mighell, and F. A. Mauer, Acta Cryst. **23**, 135 [1967].
[6] A. D. Mighell, C. W. Reimann, and A. Santoro, Acta Cryst. **B25**, 595 [1967].
[7] J. Reedijk, B. A. Stork-Blaisse, and G. C. Verschoor, Inorg. Chem. **10**, 2594 [1971].
[8] J. Reedijk, Rec. Trav. Chim. **89**, 605 [1970].
[9] M. T. Hutchings, Solid State Physics **16**, 227 [1964].
[10] S. Sugano, Y. Tanabe, and H. Kamimura, Multiplets of Transition Metal Ions in Crystals, Academic Press, New York 1970.
[11] A. Vermaas, W. L. Groeneveld, and J. Reedijk, Z. Naturforsch. **32a**, 632 [1977].
[12] A. Vermaas, unpublished results.
[13] R. W. Balk, internal report, Department of Coordination Chemistry, State University Leiden.
[14] J. Reedijk, Rec. Trav. Chim. **88**, 1451 [1969].
[15] R. L. Collins, J. Chem. Phys. **42**, 1072 [1965].
[16] J. van Dongen Torman, R. Jagnnathan, and J. M. Trooster, Hyperfine Interactions **1**, 135 [1975].
[17] M. A. Porai-Koshits and A. S. Antsishkina, Soviet Phys. Cryst. **3**, 694 [1958].